Journal of Applied Electrochemistry (2006) 36:899–905
DOI 10.1007/s10800-006-9147-6

Effects of structure of the ionic head of cationic surfactant on its inhibition of acid corrosion of mild steel

MAHMOUD M. SALEH[1,*] and ASEM A. ATIA[2]
[1]*Chemistry Department, Faculty of Science, Cairo University, Cairo, Egypt*
[2]*Department of Chemistry, Faculty of Science, Menofia University, Menofia, Egypt*
*(*author for correspondence, e-mail: mahmoudsaleh90@yahoo.com)*

Received 22 November 2005; accepted in revised form 8 April 2006

Key words: corrosion, inhibitor, quaternary, steel, surfactant

Abstract

Two *n*-alkyl-quaternary ammonium compounds were studied as corrosion inhibitors for acid corrosion of mild steel using electrochemical and weight loss methods. The two compounds are hexadecylpyridinium bromide (HDPB) and hexadecyltrimethyl ammonium bromide (HDTB). The influence of the structure of the ionic head on the inhibition action of the two cationic surfactants was studied by analyzing the data at different concentrations and temperatures. The inhibition efficiency increases with the concentration. It increases with temperature in the case of HDPB but decreases in the case of HDTB. The apparent activation energy, E_a of corrosion in the presence of HDPB was found to be lower than in blank (0.5 M H_2SO_4). In the case of HDTB, E_a was larger than that of the blank. A larger extent of adsorption for HDPB on the metal surface was evident from the larger negative values of the free energy of adsorption. The results yielded the extent and mode of adsorption of the inhibitors on mild steel. The stronger adsorption of HDPB was attributed to the differences in the molecular structures of the inhibitors.

1. Introduction

Different categories of organic compounds have been used as corrosion inhibitors in industrial acid cleaning, acid pickling and acid de-scaling to control acid corrosion of metals [1, 2]. Long chain *n*-alkyl-quaternary ammonium compounds (QA) have been used as inhibitors for acid corrosion of steels in HCl and H_2SO_4 solutions [3–6]. These compounds inhibit mainly by surface adsorption. The molecular structure of QA, the solution composition and the nature of the metal surface define the mode and extent of adsorption and hence the efficiency of such inhibitors. As the molecular structure of such compounds has a positively charged $-N^+$ ion they undergo electrostatic attraction to the induced negative charges on the iron surface. This behavior, however, was found to be different with different structure of the ionic head. It has been reported that heterocyclic systems bearing a quaternized nitrogen atom give better corrosion inhibition than the alkyl substituted quaternary ammonium compounds [7, 8]. In this case chemical adsorption is proven between the QA molecule via the heterocyclic π-electrons and the empty low-energy d-orbital of the Fe atoms [9]. Also, the number of carbon atoms in the alkyl chain carbon length is known to increase corrosion inhibition [10, 11]. The action of the long alkyl chain is to stabilize the adsorption of the ionic group on the metal surface through Van der Waals forces. Study of the inhibition actions of *n*-alkyl-quaternary ammonium compounds on the corrosion of steels is of considerable interest due to its academic and industrial importance.

It is the aim of the present work to study the effects of the structure of the ionic head of hexadecylpyridinium bromide and hexadecyltrimethyl ammonium bromide on the corrosion inhibition of mild steel in 0.5 M H_2SO_4 solution. Polarization curves are collected at different inhibitor concentrations and different temperatures. Weight loss measurements are obtained to confirm the electrochemical results. Also the mode and extent of adsorption is explained in the light of adsorption isotherms.

2. Experimental

The inhibitors; hexadecylpyridinium bromide (HDPB) and hexadecyltrimethyl ammonium bromide (HDTB) were obtained from Aldrich and used as received. The structure formulae of the surfactants are shown in Figure 1. Stock solutions were prepared in 0.5 M H_2SO_4 and the desired concentrations were obtained by appropriate dilution. De-ionized water was used in preparation of the solutions. The temperature was adjusted to ±0.2 °C using a water thermostat.

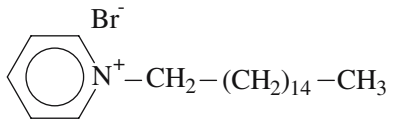

Hexadecylpyridinium bromide (HDPB)

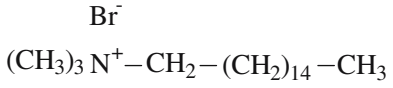

Hexadecyltrimethyl bromide (HDTB)

Fig. 1. The structure formulae of the surfactants.

Iron samples had a composition of 0.15% C, 0.27% Mn, 0.06% Si, 0.01% S, 0.015% P and the remainder iron. The iron sample was polished gradually with wet SiC paper down to 00 grade. It was then washed with bidistilled water and finally degreased by rinsing with acetone and dried. Weight loss measurements were achieved on circular iron discs of 1.8 cm diameter and thickness 0.5 cm. Two samples were immersed in 100 ml of the corroding solutions for 1 h. The rate of corrosion in the absence and presence of the surfactant was determined for each sample and the mean value was taken.

Electrochemical measurements were performed using an EG&G Princeton Applied Research Model 263A potentiostat/galvanostat controlled by m352 electrochemical analysis software. Polarization experiments were carried out in a conventional three-electrode cell. The iron electrode was fitted into a glass tube of appropriate internal diameter by using epoxy resins. The exposed surface area of the electrode was 0.50 cm^2. The counter electrode was made of a platinum sheet and the reference electrode was of the type Ag/AgCl/KCl (sat.) with a Luggin probe placed close to the electrode surface. The iron electrode was immersed for 30 min at the free corrosion potential, E_{cor}, in the solution before the polarization curves were recorded. The polarization curves were recorded potentiodynamically with a constant scan rate of 1 mV s^{-1}. Current densities were calculated on the basis of the apparent surface area of the electrode. The measurements were repeated to test the reproducibility of the results.

The critical micelle concentration (cmc) of HDPB was determined using conductivity measurements. Different solutions of HDPB in 10^{-3} M H_2SO_4 were prepared and its molar conductivities were determined from the conductivity measurements which were obtained using a conductivity meter of the type Jenway (UK) 4010. Figure 2 shows the plots of the molar conductivity against HDPB concentration. The arrow in the figure points to the cmc. The temperature does not have significant effects on the cmc of HDPB under the prevailing conditions. A similar value was estimated for the other surfactant; HDTB. The concentration of

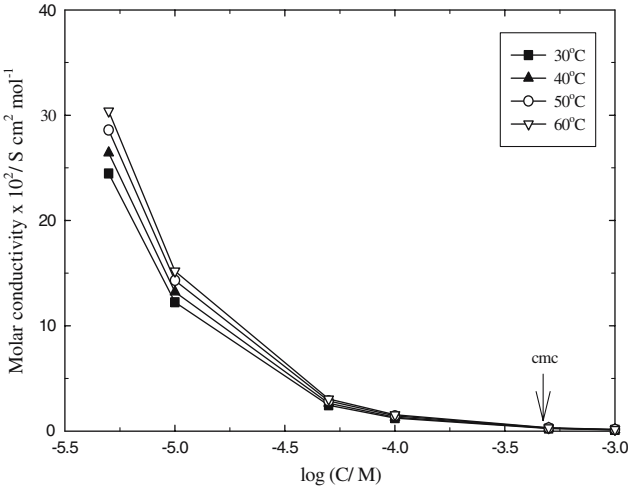

Fig. 2. Molar conductivity measurements of HDPB at different temperatures.

H_2SO_4 of 10^{-3} M was suitable for the conductivity measurements.

3. Results and discussion

3.1. *Polarization curves*

Figures 3, 4 show polarization curves for iron in the absence and presence of 1×10^{-4} M of HDPB and HDTB in 0.5 M H_2SO_4 at 30 and 60 °C, respectively. The inhibitors shift both the anodic and cathodic Tafel lines to lower current values. This indicates that both inhibitors affect both the anodic and cathodic reaction; they act as mixed-type inhibitors. The shifts for HDPB are greater than for of HDTB. At 60 °C, HDPB sustains significant shifts of both Tafel lines to lower currents. On the other hand, and at this higher temperature, the other inhibitor, HDTB, shows weak influence on both

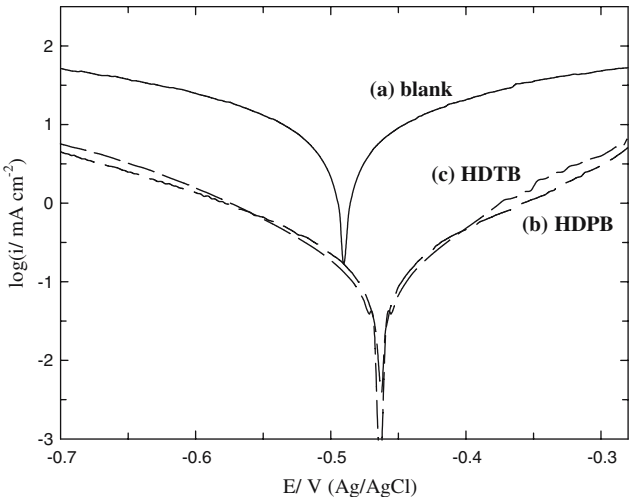

Fig. 3. Polarization curves for mild steel in different inhibitors at 30 °C. (a) Blank, 0.5 M H_2SO_4, (b) 1×10^{-4} M HDPB in 0.5 M H_2SO_4, (c) 1×10^{-4} M HDTB in 0.5 M H_2SO_4.

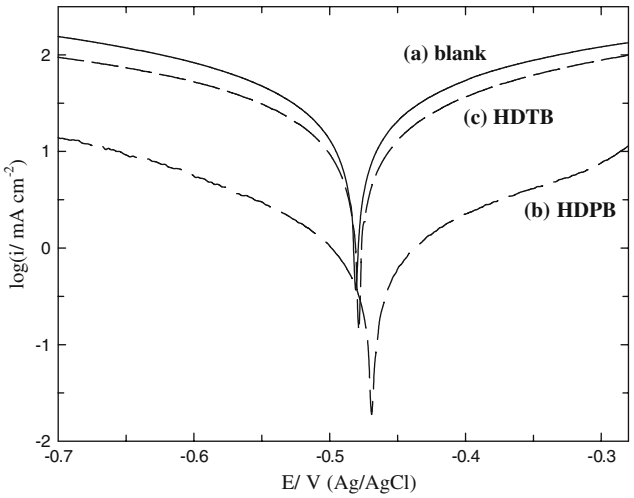

Fig. 4. Polarization curves for mild steel in different inhibitors at 60 °C. (a) Blank, 0.5 M H_2SO_4, (b) 1×10^{-4} M HDPB, (c) 1×10^{-4} M HDTB in 0.5 M H_2SO_4.

the Tafel lines. This indicates stronger inhibition of HDPB than HDTB specially at higher temperatures. The difference in molecular structures of the two inhibitors is in the ionic head. HDPB has a pyridinium ring while HDTB has 3-methyl groups attached to the quaternary ammonium atom. Similar polarization curves were collected at different inhibitor concentrations and temperatures and the above conclusions were also noted. The data from different polarization curves at 30, 40, 50 and 60 °C were analyzed to extract the important electrochemical parameters but for simplicity only those at 30 and 60 °C are shown in Table 1. The E_{cor} values are shifted anodically. The shifts depend on the inhibitor concentration and temperature. According to Riggs [12] and others [13] it is possible to classify an inhibitor as a cathodic or anodic type only if the displacement in E_{cor} (inhibitor) is at least 85 mV with respect to E_{cor} (blank). In the present study the maximum displacement is <85 mV. In the case of HDPB, although the shifts in E_{cor} are larger than in case of HDTB, they are too small to indicate that it acts as an anodic inhibitor and both inhibitors are mixed-type inhibitors under the prevailing conditions. The corrosion current, i_{cor} was determined by extrapolating the Tafel lines to the E_{cor} values. In both cases, it decreased with inhibitor concentration and increased with temperature. The anodic and cathodic Tafel slopes, B_a and B_c (not shown here), did not change in the presence of the inhibitors. This indicates that the action of both inhibitors are simple blocking of the iron surface. The values of the polarization resistance, R_p, are given in Table 1. R_p increases with inhibitor concentration and decreases with temperature. A higher value of R_p indicates a lower rate of corrosion. Also, the values for R_p of HDPB are higher than these for HDTB. The differences are more pronounced at higher temperatures.

3.2. *Weight loss results*

The inhibition efficiency, IE_w, was calculated by using the corrosion rates obtained from the weight loss measurements using the equation

$$IE_w = 100x\left[\frac{r_o - r_{inh}}{r_o}\right], \quad (1)$$

where r_{inh} and r_o are the corrosion rates in the presence and absence of the inhibitor, respectively. The IE_w values at 30 and 60 °C and at different inhibitor concentrations are listed in Table 2. In both cases IE_w increases with inhibitor concentration. At 60 °C the situation is different. HDPB has a higher IE_w but HDTB has lost inhibition efficiency. This is in accordance with the results obtained from the polarization curves.

3.3. *Effects of temperature*

The effects of temperature on the electrochemical parameters are shown in Table 1. Of interest here is

Table 1. Electrochemical parameters for mild steel in 0.5 M H_2SO_4 at different concentrations and temperatures for HDPB and HDTB

Inhibitor		HDPB			HDTB		
T/°C	C_{inh}/mol l^{-1}	E_{cor}/V (Ag/AgCl)	i_{cor}/mA cm^{-2}	R_p/ohm cm^2	E_{cor}/V (Ag/AgCl)	i_{cor}/mA cm^{-2}	R_p/ohm cm^2
30	0	−0.496	4.0	6.5	−0.496	4.0	6.5
	1×10^{-6}	−0.4920	3.3	7.0	−0.497	3.2	6.8
	5×10^{-6}	−0.488	3.0	8.2	−0.498	2.9	7.5
	1×10^{-5}	−0.4901	2.7	11.4	−0.495	2.7	12.6
	5×10^{-5}	−0.482	1.7	40.6	−0.473	1.8	35.0
	1×10^{-4}	−0.463	0.95	158	−0.463	1.3	142
	5×10^{-4}	−0.451	0.15	206	−0.461	0.98	165
	1×10^{-3}	−0.450	0.15	343	−0.463	0.98	168
60	0	−0.481	33.6	2.0	−0.481	33.6	2.0
	1×10^{-6}	−0.481	26.9	2.5	−0.481	32.6	2.2
	5×10^{-6}	−0.480	23.5	3.0	−0.481	31.9	2.5
	1×10^{-5}	−0.482	18.8	4.6	−0.479	30.9	2.7
	5×10^{-5}	−0.475	9.08	12	−0.478	26.3	2.9
	1×10^{-4}	−0.469	4.37	24	−0.478	23.2	3.5
	5×10^{-4}	−0.415	0.50	171	−0.472	20.9	5.8
	1×10^{-3}	−0.410	0.50	133	−0.466	20.2	5.7

Table 2. Weight loss measurements: corrosion rates and protection efficiency for mild steel corrosion in presence of different inhibitors in 0.5 M H_2SO_4 (A)HDPB and (B) HDTB

T/°C	Inhibitor/M	Rate of corrosion/mg cm^{-2} h^{-1}	IE_w/%
(A) HDPB			
30	Blank (0.5 M H_2SO_4)	6.15	–
	1×10^{-6}	5.25	14.5
	5×10^{-6}	4.73	23.0
	1×10^{-5}	4.24	31.0
	5×10^{-5}	2.77	55.0
	1×10^{-4}	1.48	76.0
	5×10^{-4}	0.49	92.0
	1×10^{-3}	0.49	92.0
60	Blank	58.5	–
	1×10^{-6}	47.7	18.0
	5×10^{-6}	42.4	27.5
	1×10^{-5}	33.6	42.5
	5×10^{-5}	16.9	71.0
	1×10^{-4}	7.60	87.0
	5×10^{-4}	2.05	96.5
	1×10^{-3}	1.76	97.0
(B) HDTB			
30	Blank (0.5 M H_2SO_4)	6.15	–
	1×10^{-6}	4.95	19.5
	5×10^{-6}	4.61	25.0
	1×10^{-5}	4.21	31.5
	5×10^{-5}	2.86	53.0
	1×10^{-4}	1.91	69.0
	5×10^{-4}	1.41	77.0
	1×10^{-3}	1.41	77.0
60	Blank	58.5	–
	1×10^{-6}	57.5	1.8
	5×10^{-6}	56.0	4.3
	1×10^{-5}	51.5	12.0
	5×10^{-5}	46.5	20.5
	1×10^{-4}	39.8	32.0
	5×10^{-4}	35.1	40.0
	1×10^{-3}	34.5	41.0

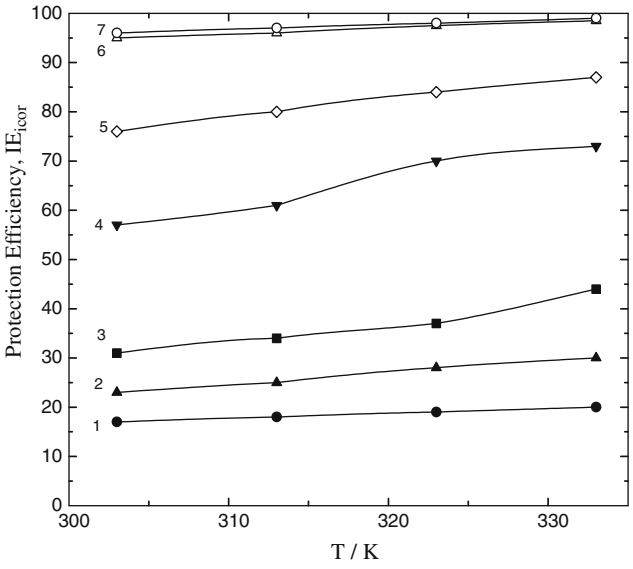

Fig. 5. Effects of temperature on $IE_{i_{cor}}$ for iron corrosion in 0.5 M H_2SO_4 at different HDPB concentrations. (1) 1×10^{-6}, (2) 5×10^{-6}, (3) 1×10^{-5}, (4) 5×10^{-5}, (5) 1×10^{-4}, (6) 5×10^{-4}, (7) 1×10^{-3} M.

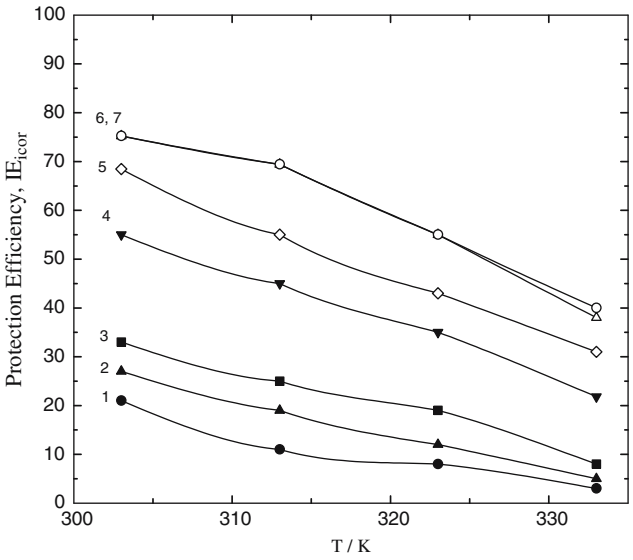

Fig. 6. Effects of temperature on $IE_{i_{cor}}$ for iron corrosion in 0.5 M H_2SO_4 at different HDTB concentrations. (1) 1×10^{-6}, (2) 5×10^{-6}, (3) 1×10^{-5}, (4) 5×10^{-5}, (5) 1×10^{-4}, (6) 5×10^{-4}, (7) 1×10^{-3} M.

comparison of the effects of temperature on the inhibition action of the two inhibitors. The inhibition efficiency, $IE_{i_{cor}}$, of the inhibitors can be calculated from i_{cor} values at different concentrations and temperatures according to an equation similar to Equation 1 but replacing r_{inh} and r_o with i_{cor2} and i_{cor1}, respectively. Note that i_{cor2} and i_{cor1} are the corrosion current densities in the presence and absence of inhibitor, respectively. Figures 5, 6 show $IE_{i_{cor}}$ at different temperature and at different concentrations of HDPB and HDTB, respectively. $IE_{i_{cor}}$ increases with the concentration of both inhibitors. It increases with temperature in the case of HDPB (Figure 5) and decreases with temperature for HDTB (Figure 6). In both cases, $IE_{i_{cor}}$ increases with inhibitor concentration until it reaches a constant value at concentration $\geq 5 \times 10^{-4}$ M, corresponding to the critical micelle concentration of the inhibitors (as shown in the experimental section). This value of cmc is comparable with literature values in similar conditions [14, 15]. In the first stage ($c < 10^{-5}$ M), the inhibitor molecules replace the adsorbed water molecules giving rise to corrosion inhibition. As the concentration increases, the inhibitor molecules replace more water molecules and the inhibition increases. At concentration near 5×10^{-4} M a bimolecular layer is formed which is stabilized by Van der Waals cohesion forces among the long chain alkyl chains which allow a more closely packed layer at the metal/solution interface. Also, the non-polar chains surrounding the positively charged nitrogen atom reduce the repulsion between ionic heads with similar charges. This allows a close packed layer to form more easily [16, 17]. At $c \geq 5 \times 10^{-4}$ M i.e., at the cmc, the

surfactant molecules tend to form micelles in solution rather than adsorbing on the iron surface and no further increase in $IE_{i_{cor}}$ was noted. The effect of temperature is different. In the case of HDPB, $IE_{i_{cor}}$ increases with temperature while for HDTB, $IE_{i_{cor}}$ decreases dramatically with temperature. The fact that the inhibiting characteristics of HDPB persist at higher temperatures may indicate chemical adsorption of HDPB on the iron surface. Also, the decrease in the inhibition efficiency with temperature for HDTB, may indicate physical adsorption of the HDTB on the iron surface [18–20].

Estimation of the apparent activation energy, E_a, in the presence and absence of the inhibitor gives valuable additional information. Arrhenius plots were used to estimate E_a. A plot of log i_{cor} against $1000/T$ gives a slope allowing calculation of E_a. The plots are shown in Figure 7 for the blank, HDPB and HDTM. The calculated E_a values are 59, 33 and 80 kJ mol^{-1} for the blank, HDPB and HDTB, respectively. The concentration of maximum $IE_{i_{cor}}$ was used here, i.e., $c = 5 \times 10^{-4}$ M of both HDPB and HDTB. The value of activation energy of corrosion in the blank solution is comparable to literature values [21, 22]. The lowering of E_a in presence of HDPB suggests chemical adsorption of the inhibitor on the iron surface. On the other hand, the higher value of E_a in the presence of the other inhibitor, HDTB, suggests physical adsorption [18–20].

3.4. *Adsorption isotherms*

Adsorption of the inhibitor molecules on the metal surface is a substitutional process since it is accompanied by exchange of adsorbed water molecules with an organic molecule. Applying an adsorption isotherm helps to estimate important thermodynamic parameters of the adsorption process. The degree of surface coverage, θ, of the metal surface was calculated from the following relation at constant potential

$$\theta = \left(\frac{i_1 - i_2}{i_1}\right), \tag{2}$$

where i_1 and i_2 are the current densities for the blank and inhibited solutions, respectively. In our case the currents were taken at a specific anodic potential of −0.35 V. Several adsorption isotherms were applied to fit the surface coverage values at different inhibitor concentrations and temperatures. The Bockris–Swinkels isotherm was found to fit with the HDPB data while the Dhar–Flory–Huggins isotherm was found to fit the HDTB data. The two isotherms are given, respectively, as [23, 24]

$$\frac{\theta}{(1-\theta)^n}\frac{[\theta + n(1-\theta)]^{(n-1)}}{n^n} = KC_{\text{inh}}, \tag{3}$$

$$\frac{\theta}{[e^{(n-1)}(1-\theta)^n]} = KC_{\text{inh}}, \tag{4}$$

where

$$K = \frac{1}{55.4}\exp\left(-\frac{\Delta G^{\circ}_{\text{ads}}}{RT}\right), \tag{5}$$

where C_{inh} is the concentration of the inhibitor in the bulk of solution, $\Delta G^{\circ}_{\text{ads}}$ is the free energy of adsorption. n represents the number of water molecules replaced by one inhibitor molecule. The isotherms were given by plotting the l.h.s of Equations 3 and 4 ($F(\theta)$) with log C_{inh}. Figure 8 shows the Bockris–Swinkels isotherm at different temperatures for HDPB. Straight lines were obtained by using a value of $n = 3$. Figure 9 shows the Dhar–Flory–Huggins isotherm at different temperatures by using a value of $n = 3$. This n value is supported by

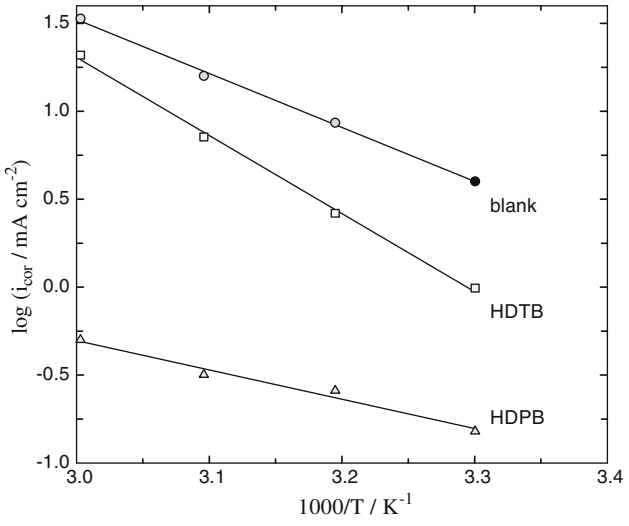

Fig. 7. Arrhenius plots for the corrosion current of mild steel in blank (0.5 M H_2SO_4), 5×10^{-4} M HDPB in 0.5 M H_2SO_4 and 5×10^{-4} M HDTB in 0.5 M H_2SO_4.

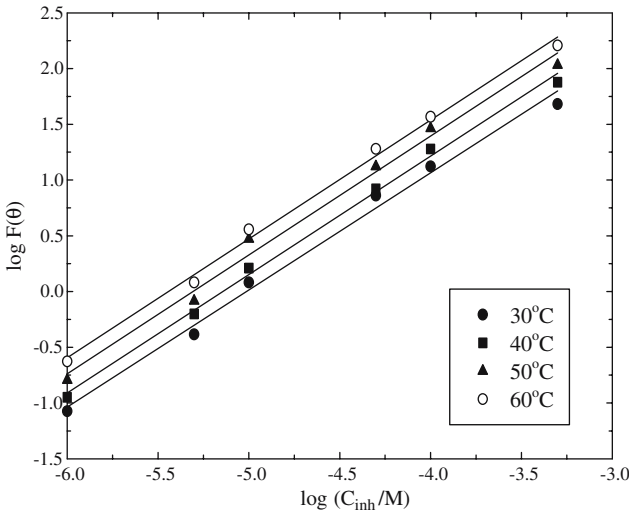

Fig. 8. Bockris–Swinkels Isotherm for HDPB at different temperatures.

literature as follows. The results of adsorption of HDPB and HDTB on silica in aqueous electrolytes showed that the areas of the ionic heads were 3.5×10^{-19} and 3.3×10^{-19} m^2, respectively [25]. Taking the area of one water molecule as 1.2×10^{-19} m^2 [26] and considering the above values of the ionic head areas can allow us to take the molecular ratio n as 3. Thus, one inhibitor molecule replaces three water molecules. The slope for HDPB is 1.0 ± 0.05 while that for HDTB is 0.95 ± 0.02 which is satisfactory for the purpose of the present study. ΔG^{o}_{ads} values were obtained at different temperatures from the intercepts in Figures 8, 9. The ΔG^{o}_{ads} values for HDPB and HDTB were plotted as a function of T as shown in Figure 10. From the slopes of Figure 10, heats of adsorption, ΔH^{o}_{ads}, for each inhibitor were determined from the basic equation, $\Delta G^{o}_{ads} = \Delta H^{o}_{ads} - T\Delta S^{o}_{ads}$. The values of heat of adsorption, ΔH^{o}_{ads} are 40.0 and -61.0 kJ mol^{-1} for HDPB and HDTB, respectively. The above results suggested stronger adsorption of HDPB than HDTB on iron [19].

Since the two compounds have the same number of carbon atoms in the alkyl chain, the different inhibition behavior is attributable to the nature of the ionic heads. The mode of adsorption of HDTB on the iron surface is via electrostatic attraction between the $HDTB^+$ cation and the induced negative charges on the iron surface. The specific adsorption of the halide ion (Br^- in our case) enhances the adsorption of the $HDTB^+$ cation by the well known synergistic effect [27, 28]. The adsorption of HDPB on the iron surface is by charge transfer bonding between the π-electrons of the pyridinium ring and the empty d-orbital of the Fe-atoms [18, 29]. There is also a strong possibility of co-adsorption of the positive cation through its $-N^+$ with the adsorbed Br^- ions on the iron surface [27, 28].

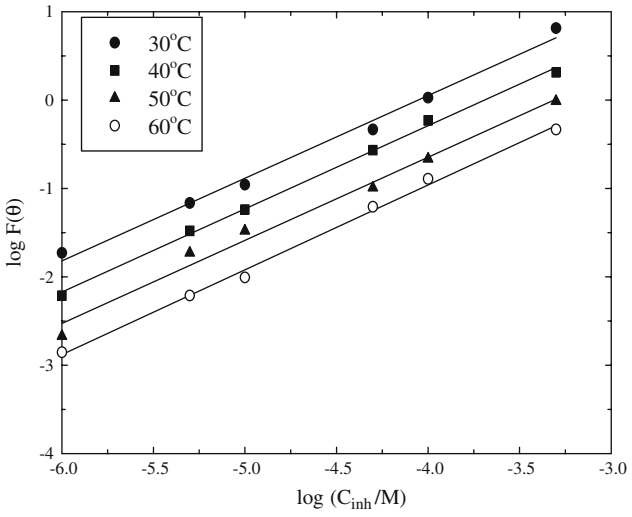

Fig. 9. Dhar–Flory–Huggins Isotherm for HDTB at different temperatures.

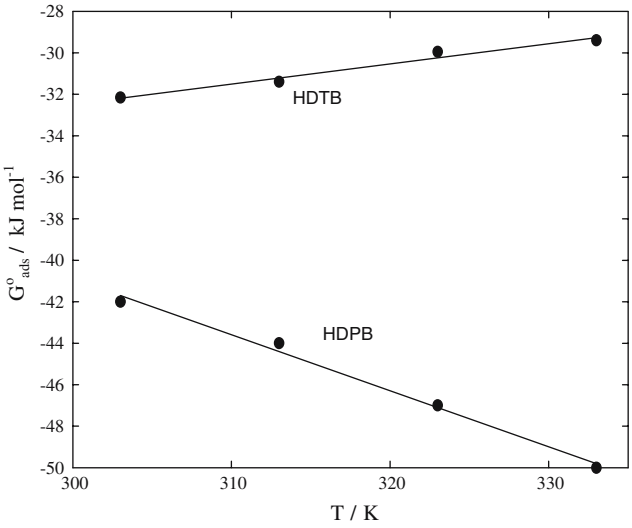

Fig. 10. Free energy of adsorption of HDPB and HDTB at different temperatures.

4. Conclusions

Two *n*-alkyl quaternary ammonium compounds were compared for their inhibition action on the corrosion of steel in 0.5 M H_2SO_4. The alkyl chain was the same in the two compounds but they were different in the structure of the ionic head. The inhibition efficiency was studied at different concentrations and at different temperatures. Efficiency increases with concentration of both inhibitors. The effect of temperature is different. In the case of HDPB, IE increases with temperature and in the case of HDTB it decreases with temperature. Surface coverage data for HDPB were fitted with the Bockris–Swinkels isotherm while HDTB data were found to fit the Dhar–Flory–Huggins isotherm. From thermodynamic parameters it is concluded that HDPB has better inhibition action than HDTB under the prevailing conditions. Chemical adsorption was suggested for HDPB and physical adsorption for HDTB because of the different chemical structures.

References

1. V.S. Sastri, *Corrosion Inhbitors; Principles and Applications* (John Wiley and Sons, NY, 1998).
2. G. Schmitt, *Br. Corr. J.* **19** (1984) 165.
3. Ling-Guang Qiu, An-Jian Xie and Yu-Hua Shen, *Corr. Sci.* **47** (2005) 273.
4. M.M. Osman, *Anti-corr. Meth. Mat.* **45** (1998) 176.
5. A. Frignani, M. Tassinari, C. Monticelli and G. Trabanelli, *Werkst. Korros.* **42** (1991) 208.
6. R. Driver and R.J. Meakins, *Br. Corr. J.* **12** (1977) 46.
7. E.A. Noor, *Corr. Sci.* **47** (2005) 33.
8. A. Frignani, C. Monticelli, G. Brunoro and G. Trabanelli *in*: Proceeding of the 6th European Symposium on Corrosion Inhibitors (Ann Univ. Ferrara, N. S., Sez. V., Suppl 8, 1985) p. 1519.
9. A.A. Atia and M.M. Saleh, *J. Appl. Electrochem.* **33** (2003) 171.
10. I. Lukouits, E. Kalman and F. Succhi, *Corrosion* **57** (2001) 3.
11. A. Bachir, A. Shiri, F. Dabosi, Y. Derbali and M. Etman, *J. Appl. Electrochem.* **21** (1991) 261.

12. O.L. Riggs Jr. *Corrosion Inhibitors*, 2nd ed., (C.C. Nathan, Houston, TX, 1973).
13. E.S. Ferreira, C. Giancomelli, F.C. Giacomelli and A. Spinelli, *Mater. Chem. Phys.* **83** (2004) 129.
14. M.M. Saleh and A.A. Atia, *Ads. Sci. Technol.* **17** (1999) 53.
15. D. Myer, *Surfactants Science and Technology* (VCH, New York, 1988).
16. R. Driver and R.J. Meakins, *Br. Corr. J.* **9** (1997) 428.
17. R. Driver and R.J. Meakins, *Br. Corr. J.* **15** (1989) 128.
18. A. Popova, E. Sokolova, S. Raicheva and M. Christov, *Corr. Sci.* **45** (2003) 33.
19. S. Sankarapapavinasam, F. Pushpanadan and M.F. Ahmed, *Corr. Sci.* **32** (1991) 193.
20. F. Bentiss, M. Traisnel and M. Lagrenee, *J. Appl. Electrochem.* **31** (2001) 41.
21. T. Szauer and A. Brandt, *Electrochim. Acta* **26** (1981) 1219.
22. B.E. El-Anadouli, B.G. Ateya and F.M. El-Nizamy, *Corr. Sci.* **26** (1986) 419.
23. J.O'M. Bockris and D.A.J. Swinkels, *J. Electrochem. Soc.* **111** (1964) 736.
24. J.M. Bastidas, P. Pinilla, E. Cano, J.L. Polo and S. Miguel, *Corr. Sci.* **45** (2003) 427.
25. D.N. Rubingh, M. Paul Holland '*Cationic Surfactants*', Vol. 37 (Marcel Dekker, New York, 1990), pp. 115–116.
26. B.G. Ateya, B.E. El-Anadouli and F.M. El-Nizamy, *Corr. Sci.* **24** (1984) 509.
27. D.P. Schweinsberg and V. Ashworth, *Corr. Sci.* **28** (1988) 539.
28. L. Larabi, Y. Harek, M. Traisnel and A. Mansri, *J. Appl. Electrochem.* **34** (2004) 833.
29. S. Kertit, J. Aride, A. Ben-Bachir, A. Srhiri and M. Etman, *J. Appl. Electrochem.* **23** (1993) 1132.